Electronic Supporting Information (ESI)

Chemomechanics in Ni–Mn Binary Cathode for Advanced Sodium-Ion Batteries

Hyungjun Kim[a‡], Myungkyu Kim[a‡], Shidong Park[a], Maenghyo Cho[a*] and Duho Kim[b*]

[a.] *Department of Mechanical Engineering, Seoul National University, 1 Gwanak-ro, Gwanak-gu, Seoul 08826, Republic of Korea.*
E-mail: mhcho@snu.ac.kr
[b.] *Department of Mechanical Engineering (Integrated Engineering Program), Kyung Hee University, 1732, Deogyeong-daero, Giheung-gu, Yongin-si, Gyeonggi-do, 17104, Republic of Korea*
E-mail: duhokim@khu.ac.kr

[‡] *These authors contributed equally*

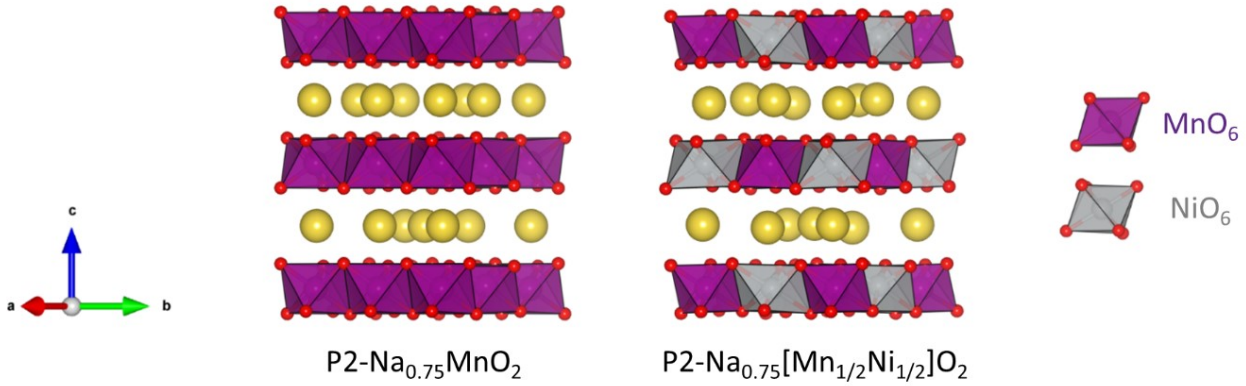

Figure S1. The atomic structures of P2-$Na_{0.75}MnO_2$ (left) and $Na_{0.75}[Mn_{1/2}Ni_{1/2}]O_2$ (right). TM layers in $Na_{0.75}MnO_2$ and $Na_{0.75}[Mn_{1/2}Ni_{1/2}]O_2$ are constituted by MnO_6 (purple octahedra) and MnO_6/NiO_6 (gray octahedra), respectively.

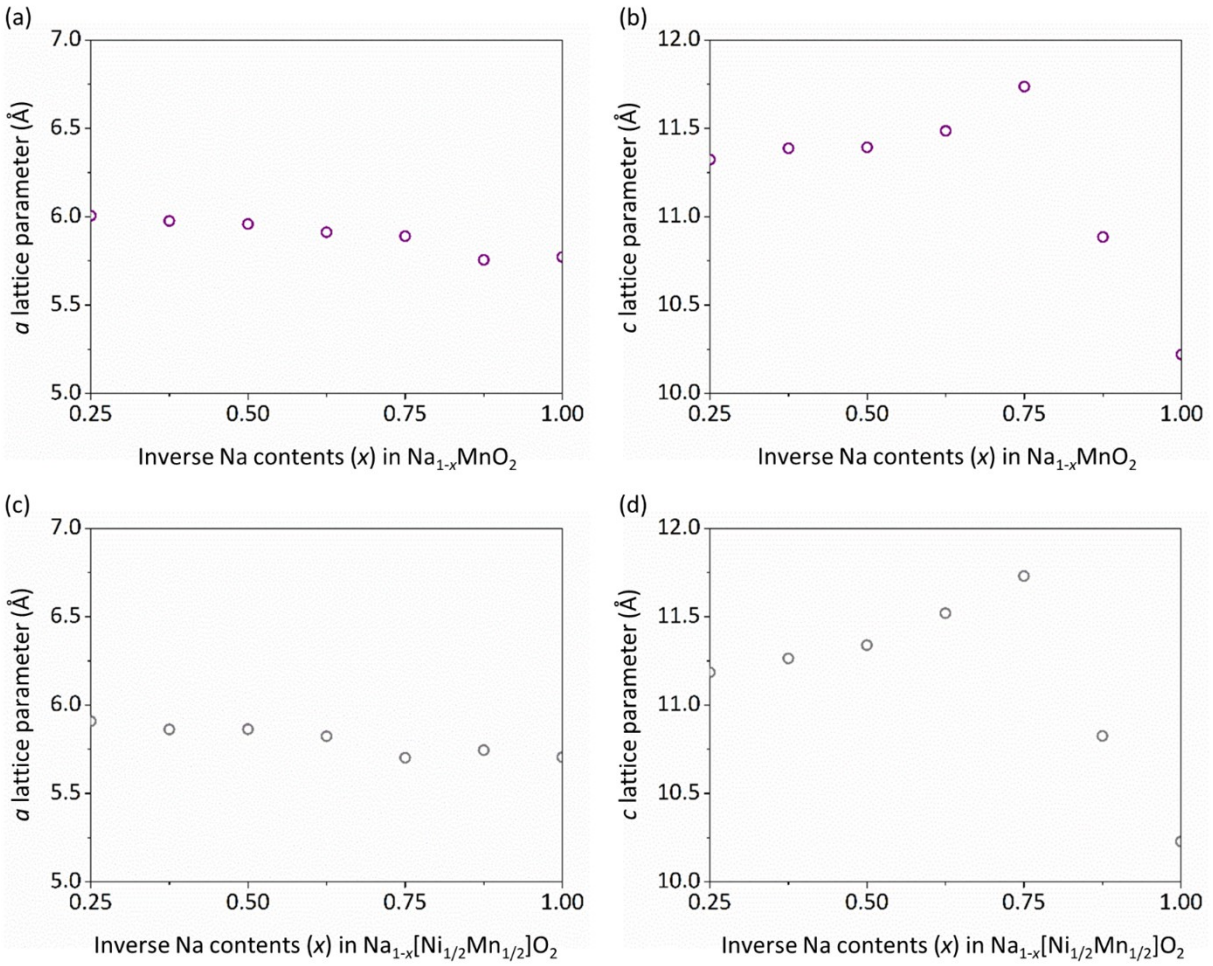

Figure S2. Calculated *a* and *c* lattice parameters with varying vacancy content (*x*) in (a-b) $Na_{1-x}MnO_2$ and (c-d) $Na_{1-x}[Mn_{1/2}Ni_{1/2}]O_2$ over the full range ($0.25 \leq x \leq 1.0$). *a* lattice parameters were calculated based on the average values of *a* and *b* lattice parameters at each vacancy content.

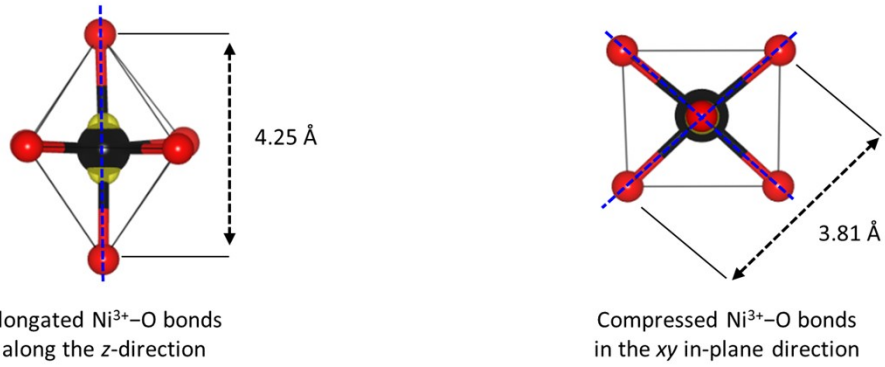

Figure S3. $Ni^{3+}O_6$ representing $Ni^{3+}O_6$ octahedra in $Na_{0.5}[Mn_{1/2}Ni_{1/2}]O_2$. The electron densities around Ni^{3+} atom are drawn in yellow. The spatial electron densities surrounding oxygen atoms are omitted. Blue dashed lines indicate the direction of O–Ni^{3+}–O configurations consisting of $Ni^{3+}O_6$. The long O–Ni^{3+}–O bond (left) shows the elongation of Ni^{3+}–O bonds along *z*-direction, whereas short ones (right) does the compression of Ni^{3+}–O bonds in the *xy* in-plane direction (right).

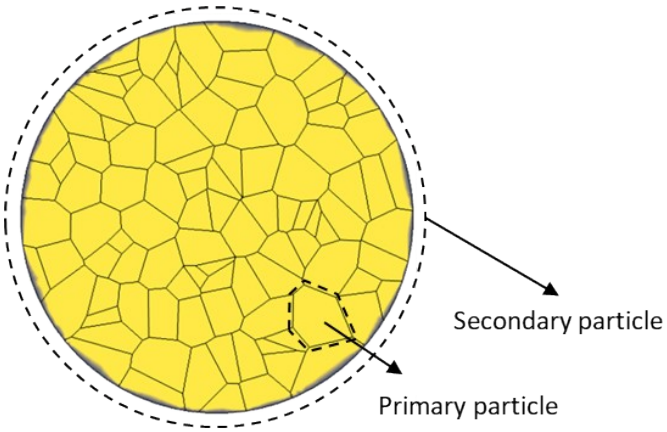

Figure S4. Illustration of primary and secondary particles.

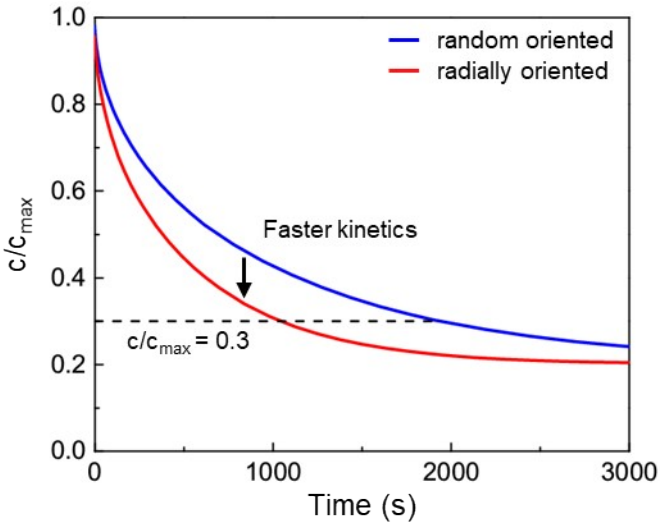

Figure S5. Na ions concentration change over time for the randomly oriented (blue) and the radially oriented (red) secondary particle during desodiation.

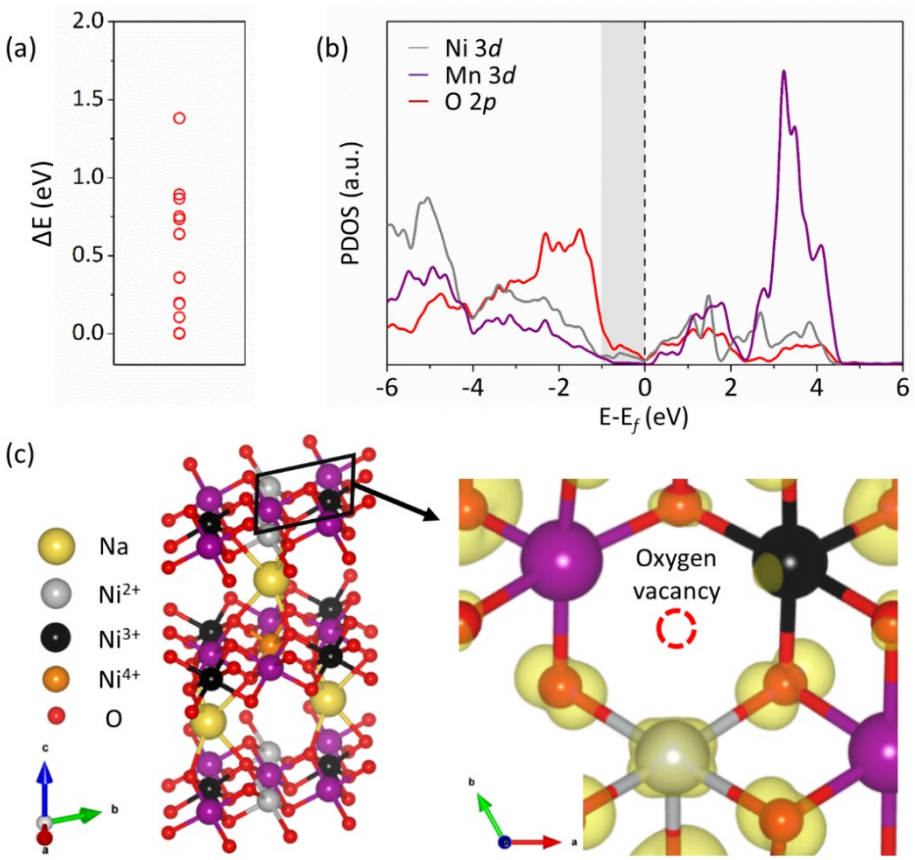

Figure S6. (a) The energy configuration of $Na_{0.25}[Mn_{1/2}Ni_{1/2}]O_2$ with a oxygen vacancy ($Na_{0.25}[Mn_{1/2}Ni_{1/2}]O_{1.875}$) corresponding to the high-voltage phase.[1] Based on the $Na_{0.25}[Mn_{1/2}Ni_{1/2}]O_{1.875}$ with the lowest formation energy, we constructed (b) combined graphs of PDOSs of Mn (purple) and Ni (gray) 3*d*-electron and O (red) 2*p*-electron and (c) calculated the spatial electron densities (yellow iso-surface) at $-1.0 \le E\text{-}E_f \le 0.0$. Red dashed circle highlights that Ni^{3+} and Ni^{4+} ions in $Na_{0.25}[Mn_{1/2}Ni_{1/2}]O_2$ are reduced to the Ni^{2+} and Ni^{3+}, respectively, as oxygen vacancy is introduced.

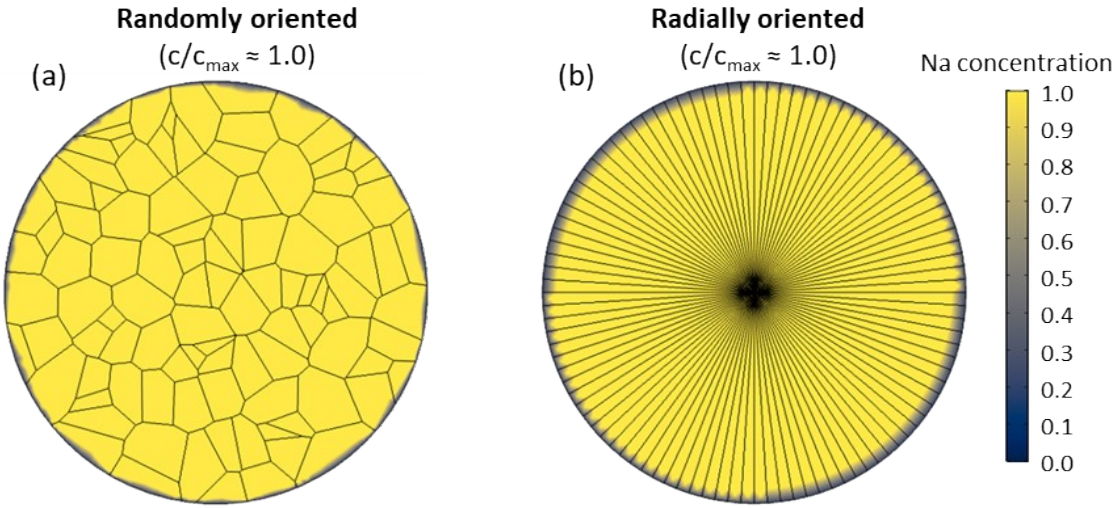

Figure S7. Concentration of Na ions for (a) the randomly oriented and (b) the radially oriented shape secondary particles at c/c_{max} ≈ 1.0.

Parameter		Value
Particle radius		5 μm
Maximum Na concentration		58418 mol/m^3
Na diffusivity along *the ab* plane		$7x10^{-15}$ m^2/s
Na diffusivity along *the c* lattice direction		$7x10^{-16}$ m^2/s
Elastic constants	C_{11}	222 GPa
	C_{12}	77 GPa
	C_{13}	36 GPa
	C_{33}	245 GPa
	C_{44}	26 GPa
	C^{66}	72.5 GPa

Table S1. Parameters used in the finite element analysis.

References

1 D. Kim and J. Lee, *Chem. Mater.*, 2020, **32**, 5541–5549.